Chapter 5
Estimation of the Buried Model Parameters from the Self-potential Data Applying Advanced Approaches: A Comparison Study

Mahmoud Elhussein and Khalid S. Essa

Abstract A comparison study using the least-squares minimization method, particle swam optimization method, and neural network method for interpreting self-potential data for typical shaped-models (spheres and cylinders). This interpretation process contains the delineation buried sources parameters, which are the amplitude factor, the depth to the structure, the source origin location, the angle of polarization, the shape factor. The stability of the suggested methods was tested on two synthetic data with and without noise and real data set from USA. The methods estimate the different structures parameters efficiently and accurately.

Keywords Self-potential data · Least-squares · Particle swarm · Neural network

5.1 Introduction

Self-potential method can be considered as one of the most effective geophysical techniques in solving different geophysical problems (Sundararajan et al. 1998; Drahor 2004; Mehanee 2014; Essa 2020; Elhussein 2020). Self-potential anomalies produced by natural potential difference which resulted due to the oxidation-reduction process of mineralized rocks which in contact with the ground water (Essa et al. 2008; Essa 2020).

To apply the self-potential technique in solving the different geophysical problems, the different subsurface geological bodies was approximated to simple geometrical bodies (like, sphere, cylinder and thin sheet) (Essa 2011; Mehanee 2014, 2015; Biswas 2017; Essa and Elhussein 2017; Sungkono and Warnana 2018; Essa 2020). To estimate the different parameters (like, amplitude coefficient, depth, polarization angle and body origin), different techniques were created and developed to overcome the ill-posedness and non-uniqueness problems (Tarantola 2005; Sharma and Biswas 2013; Essa 2019). From these techniques, gradient techniques (Abdelrahman et al. 2004, 2009b; Essa and Elhussein 2017), moving average techniques (Abdelrahman et al. 2006a; Mehanee et al. 2011; Essa 2019), characteristic curves and nomograms

M. Elhussein · K. S. Essa (✉)
Faculty of Science, Geophysics Department, Cairo University, Giza 12613, Egypt

A. Biswas (ed.), *Self-Potential Method: Theoretical Modeling and Applications in Geosciences*, Springer Geophysics, https://doi.org/10.1007/978-3-030-79333-3_5

(Yungul 1950; Fitterman 1979; Essa 2007; Abdelrahman et al. 2009a), nonlinear and liner least squares techniques (Abdelrahman et al. 2006b; Essa et al. 2008), Euler deconvolution method (Agarwal and Srivastava 2009); most of the previous methods require a priori information, other methods estimate the different parameters with high uncertainty as the accuracy of the estimated parameters mainly depends upon the accuracy of the regional-residual separation. Nowadays new recent techniques have been developed, like particle swarm optimization (Essa 2019, 2020), genetic-price technique (Di Maio et al. 2019), black-hole technique (Sungkono and Warnana 2018).

This chapter review different techniques applied to the different synthetic and real field self-potential data to estimate the different bodies parameters.

5.2 Methodology

5.2.1 Forward Modeling

The SP anomaly (V) caused by simple geometrical structures at any given point (p) (Bhattacharya and Roy 1981; Essa 2019) (Fig. 5.1) is given by:

$$V\left(x_j\right) = K\frac{\left(x_j - d\right)cos\theta - zsin\theta}{\left(\left(x_j - d\right)^2 + z^2\right)^q}, \quad i = 0, 1, 2, 3, \ldots, N \tag{5.1}$$

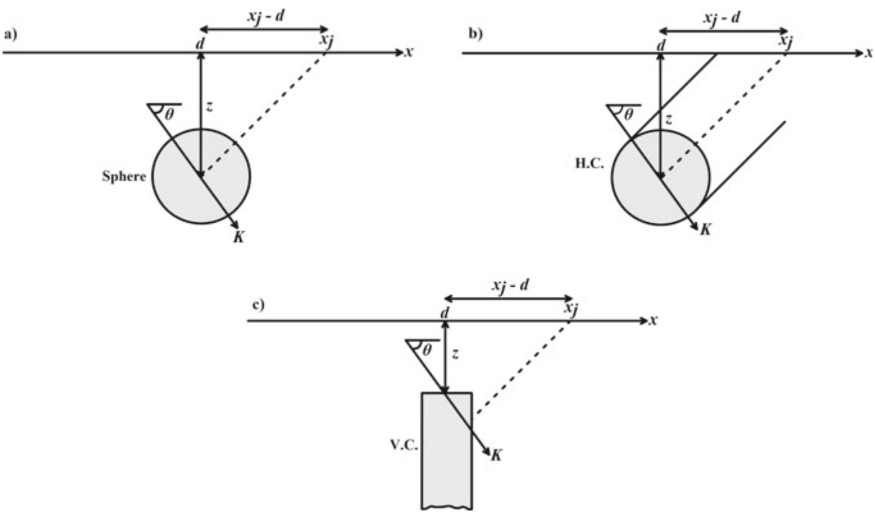

Fig. 5.1 A sketch showing the different geometrical shapes and their parameters: **a** sphere, **b** horizontal cylinder and **c** vertical cylinder

where K is the amplitude factor (mV x m^{2q-1}), z is the depth to the structure (m), d is the source origin (m), θ is the angle of polarization (degrees), q is the shape factor (dimensionless) which takes the following values: 1.5 for sphere, 1 for horizontal cylinder and 0.5 for vertical cylinder (Essa et al. 2008; Di Maio et al. 2016; Essa 2019).

5.2.2 Least Squares Inversion Technique

Essa et al. (2008) developed a least square inversion approach to estimate the different bodies parameters, by determining the depth applying the nonlinear equation:

$$\delta(z) = 0, \tag{5.2}$$

After estimating the depth, the angle of polarization is then calculated by the least square, also, the amplitude factor is then determined from the estimate depth and the polarization angle.

5.2.3 Particle Swarm Optimization

Essa (2019) developed a method based upon the PSO algorithm and the second moving average for estimating the different structures parameters. PSO is stochastic in its nature, the idea of PSO is based upon a group of birds or fishes looking for food, the group of birds represent the models, and the paths of particles represent the solutions (Essa 2019). The algorithm starts with random models, then the location and the velocity of the particles are updated using the following formulas, respectively.

$$x_i^{k+1} = x_j^k + V_j^{k+1} \tag{5.3}$$

$$V_j^{k+1} = c_3 V_j^k + c_1 rand\left(T_{best} - x_j^{k+1}\right) + c_2 rand\left(J_{best} - x_j^{k+1}\right), \tag{5.4}$$

where x_j^k is the location of jth particle at the iteration kth; V_j^k is the velocity of the jth model at the iteration kth; *rand* is any random number between [0, 1]; c_1 and c_2 are cognitive and social factors and equal 2 (Parsopoulos and Vrahatis 2002; Singh and Biswas 2016; Essa 2019); c_3 is the inertial coefficient which governs the velocity of the model and usually takes a value less than one; T_{best} is the best location for individual model, and J_{best} is the global best location for any model in the group.

5.2.4 Neural Network Algorithm

Al-Garni (2009) proposed an approach based mainly on neural network (modular algorithm) to estimate the different structures parameters.

5.3 Synthetic Examples

5.3.1 Sphere Model

A noise free SP anomaly was generated using sphere model with the following parameters: K = 1200 mV x m^2, z = 6, $\theta = 45°$, d = 55 m, q = 1.5 and the profile length = 100 m (Fig. 5.2).

The different previous techniques were applied to estimate the different parameters. First the least square inversion technique was applied to the SP profile and the parameters were estimated accurately with no error (Table 5.1), then the PSO technique produce the parameters with 0% error (Table 5.1), Finally, the data were subjected to neural network and the parameters were estimated efficiently (Table 5.1).

To test the effect of noisy data on the different techniques, a 10% random noise was added to the previous SP model. For least square inversion technique, the estimated parameters are: K = 1020 mV x m^2, z = 6.5, $\theta = 47°$; while for PSO technique, the estimated parameters are: K = 1140 mV x m^2, z = 5.8, $\theta = 44.5°$, d = 54.9 m, q = 1.45; and in case of neural network, the estimated parameters are: K = 1350 mV x m^2, z = 6.3, $\theta = 45.7°$, q = 1.57 (Table 5.2). The error of the estimated parameters is shown in (Table 5.2).

5.3.2 Horizontal Cylinder Model

A noise free SP anomaly was generated using horizontal cylinder model with the following parameters: K = 900 mV x m, z = 6.5, $\theta = 40°$, d = 60 m, q = 1 and the profile length = 100 m (Fig. 5.3).

The different previous techniques were applied to estimate the different parameters. First the least square inversion technique was applied to the SP profile and the parameters were estimated accurately with no error (Table 5.1), then the PSO technique produce the parameters with 0% error (Table 5.2), Finally, the data were subjected to neural network and the parameters were estimated efficiently (Table 5.2).

To test the effect of noisy data on the different techniques, a 10% random noise was added to the previous SP model. For least square inversion technique, the estimated parameters are: K = 1000 mV x m, z = 7.1, $\theta = 41.5°$; while for PSO technique,

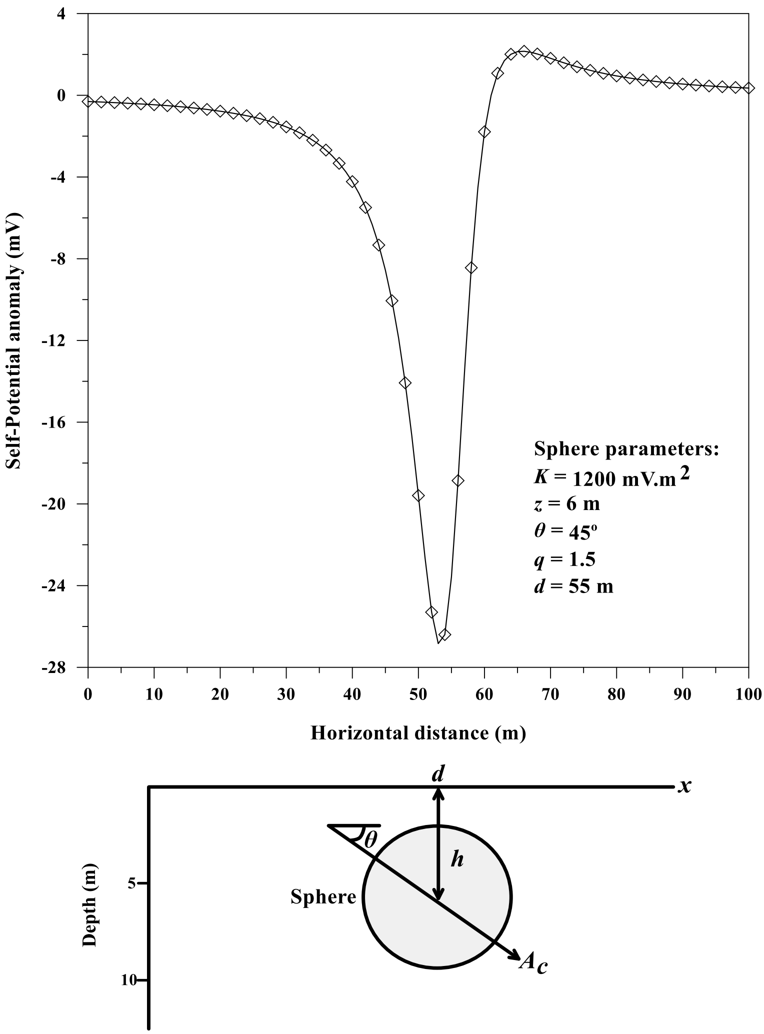

Fig. 5.2 Self-potential anomaly profile of sphere model ($K = 1200$ mV $\times$ m^2, $z = 6$ m, $\theta = 45°$, $q = 1.5$, and $d = 55$ m) and profile length 100 m

the estimated parameters are: K = 960 mV x m, z = 6.6, $\theta = 40.2°$, d = 60.11 m, q = 1.04; and in case of neural network, the estimated parameters are: K = 1010 mV x m, z = 6.3, $\theta = 39.7°$, q = 0.9 (Table 5.2). The error of the estimated parameters is shown in (Table 5.2).

Table 5.1 A correlation between results obtained from different methods applied to the self-potential anomaly of sphere model ($K = 1200$ mV $\times$ m^2, $z = 6$ m, $\theta = 45°$, $q = 1.5$, and $d = 55$ m)

Methods parameters	Essa et al. (2008) method		Al-Garni (2009) method		Essa (2019) method	
	Noise-freee					
	Results	Error (%)	Results	Error (%)	Results	Error (%)
K (mV x m^2)	1200	0	1200	0	1200	0
z (m)	6	0	6	0	6	0
θ (degree)	45	0	45	0	45	0
q (dimensionless)	–	–	1.5	0	1.5	0
d (m)	–	–	–	–	55	0
Results (after adding 10% random noise)						
	Results	Error (%)	Results	Error (%)	Results	Error (%)
K (mV x m^2)	1020	15	1350	12.5	1140	5
z (m)	6.5	8.33	6.3	5	5.8	3.33
θ (degree)	47	4.44	45.7	1.56	44.5	1.11
q (dimensionless)	–	–	1.57	4.67	1.45	3.33
d (m)	–	–	–	–	54.9	0.18

Table 5.2 A correlation between results obtained from different methods applied to the self-potential anomaly of H.C. model ($K = 900$ mV $\times$ m, $z = 6.5$ m, $\theta = 40^o$, $q = 1$, and $d = 60$ m)

Methods parameters	Essa et al. (2008) method		Al-Garni (2009) method		Essa (2019) method	
	Noise-freee					
	Results	Error (%)	Results	Error (%)	Results	Error (%)
K (mV x m)	900	0	900	0	900	0
z (m)	6.5	0	6.5	0	6.5	0
θ (degree)	40	0	40	0	40	0
q (dimensionless)	–	–	1	0	1	0
d (m)	–	–	–	–	60	0
Results (after adding 10% random noise)						
	Results	Error (%)	Results	Error (%)	Results	Error (%)
K (mV x m)	1000	11	1010	12.2	960	4
z (m)	7.1	9.23	6.3	3.08	6.6	1.54
θ (degree)	41.5	3.75	39.7	0.75	40.2	0.5
q (dimensionless)	–	–	0.9	10	1.04	4
d (m)	–	–	–	–	60.11	0.18

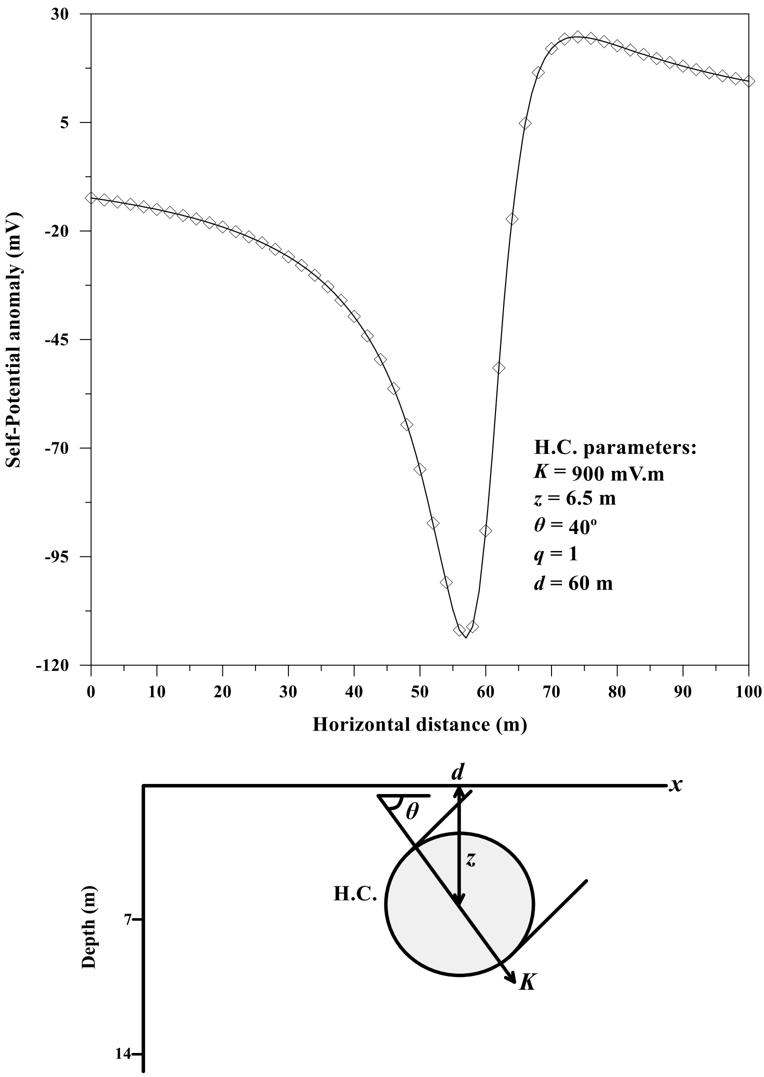

Fig. 5.3 Self-potential anomaly profile of H.C. model ($K = 900$ mV × m, $z = 6.5$ m, $\theta = 40°$, $q = 1$, and $d = 60$ m) and profile length 100 m

5.4 Field Example

5.4.1 Malachite Mine, USA Real Data

Malachite mine is composed of amphibolite belt which surrounded by gneiss and schist (Essa 2019). Self-potential profile was designed and measured by Heiland et al. (1945), the profile was taken above massive sulfide ore body which located in the Malachite mine. The profile length was 164 m, digitized at 1.25 m (Fig. 5.4). The SP profile was then subjected to the three different techniques to determine and compare between the parameters estimated from these different methods (Table 5.3). From Table 5.3 the parameters estimated using least square inversion method (Essa et al. 2008) are: $K = 275.39$ mV, $z = 12.87$, $\theta = 103.58°$; while the parameters estimated by using PSO technique (Essa 2019) are: $K = 236.53$ mV, $z = 13.74$, $\theta =$

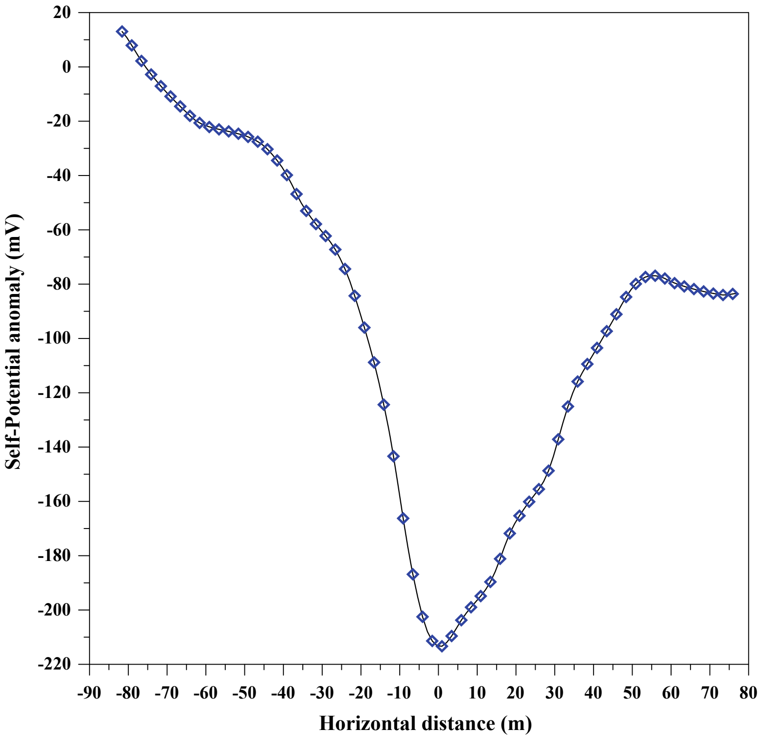

Fig. 5.4 Self-potential anomaly profile of Malachite mine, USA field example

Table 5.3 A correlation between results obtained from different methods applied to the self-potential anomaly of Malachite mine, USA field example

Methods parameters	Essa et al. (2008) method	Al-Garni (2009) method	Essa (2019) method
K (mV)	275.39	268.41	236.53
z (m)	12.87	13.2	13.74
θ (degree)	103.58	105	99.31
q (dimensionless)	–	0.63	0.45
d (m)	–	–	0.20

99.31° d = 0.20 m, q = 0.45; finally, the parameters estimated using neural network (Al-Garni 2009) are: $K = 268.41$ mV, $z = 13.2$, $\theta = 105°$, $q = 0.63$.

5.5 Conclusions

A comparative study was made in this chapter to see the differences between different methods in application to the self-potential data from different geological structures (Sphere, horizontal cylinder and vertical cylinder). the different methods are least-square (Essa 2008), neural network (Al-Garni 2009) and PSO (Essa 2019). These different methods were applied to two different synthetic data without and with 10% random noise and one real data from USA. The methods estimate the different structures parameters (K, z, d, θ and q) efficiently and accurately.

References

Abdelrahman EM, El-Araby TM, Essa KS (2009a) Shape and depth determination from second moving average residual self-potential anomalies. J Geophys Eng 6:43–52

Abdelrahman EM, Essa KS, Abo-Ezz ER, Soliman KS (2006a) Self-potential data interpretation using standard deviations of depths computed from moving average residual anomalies. Geophys Prospect 54:409–423

Abdelrahman EM, Essa KS, El-Araby TM, Abo-Ezz ER (2006b) A least-squares depth-horizontal position curves method to interpret residual SP anomaly profile. J Geophys Eng 3:252–259

Abdelrahman EM, Saber HS, Essa KS, Fouda MA (2004) A least-squares approach to depth determination from numerical horizontal self-potential gradients. Pure appl Geophys 161:399–411

Abdelrahman EM, Soliman KS, Abo-Ezz ER, Essa KS, El-Araby TM (2009b) Quantitative interpretation of self-potential anomalies of some simple geometric bodies. Pure appl Geophys 166:2021–2035

Agarwal B, Sirvastava S (2009) Analyses of self-potential anomalies by conventional and extended Euler deconvolution techniques. Comput Geosci 35:2231–2238

Al-Garni MA (2009) Interpretation of spontaneous potential anomalies from some simple geometrically shaped bodies using neural network inversion. Acta Geophys 58:143. https://doi.org/10.2478/s11600-009-0029-2

Biswas A (2017) A review on modeling, inversion and interpretation of self-potential in mineral exploration and tracing paleo-shear zones. Ore Geol Rev 91:21–56

Di Maio R, Piegari E, Rani P, Carbonari R, Vitagliano E, Milano L (2019) Quantitative interpretation of multiple self-potential anomaly sources by a global optimization approach. J Appl Geophys 162:152–163

Di Maio R, Rani P, Piegari E, Milano L (2016) Self-potential data inversion through a genetic-price algorithm. Comput Geosci 94:86–95

Drahor MG (2004) Application of the self-potential method to archaeological prospection: some case histories. Archaeol Prospect 11:77–105

Elhussein M (2020) A novel approach to self-potential data interpretation in support of mineral resource development. Nat Resour Res. https://doi.org/10.1007/s11053-020-09708-1

Essa KS (2007) Gravity data interpretation using the s-curves method. J Geophys Eng 4:204–213

Essa KS (2011) A new algorithm for gravity or self-potential data interpretation. J Geophys Eng 8:434–446

Essa KS (2019) A particle swarm optimization method for interpreting self potential anomalies. J Geophys Eng 16:463–477

Essa KS (2020) Self potential data interpretation utilizing the particle swarm method for the finite 2D inclined dike: mineralized zones delineation. Acta Geod Geophys 55:203–221

Essa KS, Elhussein M (2017) A new approach for the interpretation of self-potential data by 2-D inclined plate. J Appl Geophys 136:455–461

Essa KS, Mehanee S, Smith P (2008) A new inversion algorithm for estimating the best fitting parameters of some geometrically simple body from measured self-potential anomalies. Explor Geophys 39:155–163

Fitterman DV (1979) Calculations of self-potential anomalies near vertical contacts. Geophysics 44:195–205

Heiland CA, Tripp MR, Wantland D (1945) Geophysical surveys at the Malachite Mine. Jefferson County Colorado Amer Inst Min Metall Eng 164:142–154

Mehanee S (2014) An efficient regularized inversion approach for self-potential data interpretation of ore exploration using a mix of logarithmic and non-logarithmic model parameters. Ore Geol Rev 57:87–115

Mehanee S (2015) Tracing of paleo-shear zones by self-potential data inversion: case studies from the KTB, Rittsteig, and Grossensees graphite-bearing fault planes. Earth Planets Space 67:14

Mehanee S, Essa KS, Smith P (2011) A rapid technique for estimating the depth and width of a two-dimensional plate from self-potential data. J Geophys Eng 8:447–456

Parsopoulos KE, Vrahatis MN (2002) Recent approaches to global optimization problems through particle swarm optimization. Nat Comput 1:235–306

Sharma SP, Biswas A (2013) Interpretation of self-potential anomaly over 2D inclined structure using very fast simulated annealing global optimization: an insight about ambiguity. Geophysics 78:WB3–WB15

Singh A, Biswas A (2016) Application of global particle swarm optimization for inversion of residual gravity anomalies over geological bodies with idealized geometries. Nat Resour Res 25:297–314

Sundararajan N, Srinivasa Rao P, Sunitha V (1998) An analytical method to interpret self-potential anomalies caused by 2D inclined sheets. Geophysics 63:1551–1555

Sungkono Warnana DD (2018) Black hole algorithm for determining model parameter in self-potential data. J Appl Geophys 148:189–200

Tarantola A (2005) Inverse problem theory and methods for model parameter estimation. PA, Society for Industrial and Applied Mathematics (SIAM), Philadelphia

Yungul S (1950) Interpretation of spontaneous polarization anomalies caused by spheroidal orebodies. Geophysics 15:163–256